



ELSEVIER

Contents lists available at ScienceDirect

## Comptes Rendus Physique

www.sciencedirect.com



Thermoelectric mesoscopic phenomena / Phénomènes thermoélectriques mésoscopiques

## Thermoelectric and electrical transport in mesoscopic two-dimensional electron gases

*Transport thermoélectrique et électrique dans des gaz d'électrons bi-dimensionnels mésoscopiques*Vijay Narayan<sup>a,\*</sup>, Michael Pepper<sup>b</sup>, David A. Ritchie<sup>a</sup><sup>a</sup> Department of Physics, University of Cambridge, J J Thomson Avenue, Cambridge, CB3 0HE, UK<sup>b</sup> Department of Electronic and Electrical Engineering, University College London, Torrington Place, London, WC1E 7JE, UK

## ARTICLE INFO

## Article history:

Available online 21 August 2016

## Keywords:

Mesoscopic systems  
Seebeck coefficient  
Phase coherence

## Mots-clés:

Systèmes mésoscopiques  
Coefficient de Seebeck  
Cohérence de phase

## ABSTRACT

We review some of our recent experimental studies on low-carrier concentration, mesoscopic two-dimensional electron gases (m2DEGs). The m2DEGs show a range of striking characteristics, including a complete avoidance of the strongly localised regime even when the electrical resistivity  $\rho \gg h/e^2$ , giant thermoelectric response, and an apparent decoupling of charge and thermoelectric transport. We analyse the results and demonstrate that these observations can be explained based on the assumption that the charge carriers retain phase coherence over the m2DEG dimensions. Intriguingly, this would imply phase coherence on lengthscales of up to 10  $\mu\text{m}$  and temperature  $T$  up to 10 K, which is significantly greater than conventionally expected in GaAs-based 2DEGs. We critically assess this assumption and explore other possible explanations to the data. Such unprecedentedly large phase coherence lengths open up several possibilities in quantum information and computation schemes.

© 2016 Académie des sciences. Published by Elsevier Masson SAS. This is an open access article under the CC BY license (<http://creativecommons.org/licenses/by/4.0/>).

## R É S U M É

Nous passons en revue certains de nos travaux expérimentaux récents sur des gaz d'électrons bi-dimensionnels mésoscopiques (GE2Dm). Les GE2Dm présentent un ensemble de propriétés caractéristiques frappantes, parmi lesquelles une absence complète de régime fortement localisé, même quand la résistance électrique  $\rho \gg h/e^2$ , des réponses thermoélectriques géantes et un découplage apparent des transports de charges et thermoélectrique. Nous analysons les résultats et montrons que ces observations peuvent s'expliquer en admettant que les porteurs de charges gardent leur cohérence quantique sur une taille de l'ordre de celle du GE2Dm. Curieusement, cela impliquerait une cohérence quantique qui attendrait des dimensions de l'ordre de 10  $\mu\text{m}$  pour des températures de 10 K, ce qui excède de beaucoup ce qui est attendu pour des gaz bidimensionnels d'électrons dans l'arséniure de gallium. Nous examinons cette hypothèse avec un esprit critique et explorons d'autres explications possibles. De telles longueurs de cohérence quantique sont sans

\* Corresponding author.

E-mail addresses: [vn237@cam.ac.uk](mailto:vn237@cam.ac.uk) (V. Narayan), [michael.pepper@ucl.ac.uk](mailto:michael.pepper@ucl.ac.uk) (M. Pepper), [dar11@cam.ac.uk](mailto:dar11@cam.ac.uk) (D.A. Ritchie).

précédent et ouvrent de nombreuses possibilités concernant l'information et le calcul quantiques.

© 2016 Académie des sciences. Published by Elsevier Masson SAS. This is an open access article under the CC BY license (<http://creativecommons.org/licenses/by/4.0/>).

## 1. Introduction

The two-dimensional electron gas (2DEG) has served as one of the most versatile arenas to realise and study mesoscopic systems for over three decades now. Mesoscopic systems are systems which are comparable in spatial extent to the electronic 'phase-coherence' length  $\ell_\phi$ , i.e. the length over which the phase of the electron is completely randomised through inelastic processes. These are ideal venues to study fundamental quantum effects such as localisation, but equally, are becoming increasingly important towards the next generation of quantum-based communications and information schemes which rely on the quantum nature of charge carriers. In this context, high-quality GaAs-based 2DEGs in conjunction with state-of-the-art lithographical techniques offer immense scope to create and manipulate mesoscopic structures such as one-dimensional quantum wires [1,2] and zero-dimensional quantum dots [3,4]. However, while the electrical and thermoelectric characteristics of quantum wires and quantum dots have been intensely studied, the more basic 'mesoscopic 2DEG', i.e. a 2D phase-coherent system, has received much less attention. Typically, 2DEGs have been studied in the macroscopic limit where the system size  $L \gg \ell_\phi$ , giving rise to the so-called '2D metal-to-insulator' (MIT) transition [5–7] and integer and fractional quantum Hall effects [8,9]. In this Review we focus on some of our recent works on 2DEGs of spatial extent  $\lesssim 10 \mu\text{m}$  where both the electrical and thermoelectrical transport contain striking departures from conventional 'macroscopic' 2DEG behaviour up to temperature  $T$  as high as 10 K. These include (1) a systematic dependence of the electrical conductivity  $\sigma$  on  $L$  [10], (2) an apparent breakdown of the canonical Mott relation between  $\sigma$  and Seebeck coefficient (or thermopower)  $S$  [11], and (3) a giant enhancement in the magnitude of  $S$  [12]. In Section 4, we make a plausible case for these observations being a result of phase coherent transport. Remarkably and very surprisingly, this would imply that  $\ell_\phi$  is two orders of magnitude larger than theoretically expected [13], a point we critically discuss further in Section 4. The remainder of this Review is structured as follows: In Section 2, we describe the experimental system and the thermoelectric measurement technique, Section 3 constitutes the main body of this article where we review the experimental results, and finally in Section 4 we conclude with a discussion and mention of some of the outstanding issues.

## 2. Experimental system

The 2DEGs described here are realised in  $\delta$ -doped GaAs heterostructures in which the 2DEG forms  $\approx 300 \text{ nm}$  below the wafer surface and the dopants are situated 40 nm above the 2DEG. The as-grown mobility of the wafers was measured at 4 K to be  $212 \text{ m}^2/\text{Vs}$  at a carrier density  $n_s = 2.2 \times 10^{12} \text{ m}^{-2}$ . The mesoscopic 2DEGs (m2DEGs) shown in Fig. 1 were lithographically patterned as follows: a wet etch was used to define a long channel with width  $W$ , after which Au–Ge–Ni ohmic contacts were deposited and annealed to make contact to the buried 2DEG. Finally, Ti–Au electrodes were deposited over the channel to create a gate-defined mesoscopic region of size  $L \times W$ , where  $L$  is the length along the transport direction. A gate voltage  $V_g$  applied to the electrodes enabled the tuning of  $n_s$  in the m2DEG. The mapping from  $V_g$  to  $n_s$  was obtained by examining reflections of edge-states when the device was tuned the quantum Hall regime by applying a perpendicular magnetic field. Due to the small  $L$  ( $\lesssim 10 \mu\text{m}$ ) the electrical and thermoelectrical properties were measured in a quasi-four-terminal setup, i.e. as shown in Fig. 1, in addition to the m2DEG there are sections of ungated 2DEG between the voltage leads. These ungated regions provide an additional (series) resistance to that of the m2DEG which, however, is largely inconsequential since it is at least an order of magnitude lower than that of the m2DEG in the parameter range of interest. A detailed discussion of this can be found in Ref. [10].

Fig. 1a schematically shows the measurement setup: both electrical and thermoelectric properties were measured using AC methods. For the former, an excitation current  $I_{\text{ex}} = 100 \text{ pA}$  at a frequency  $f \sim 7 \text{ Hz}$  was used. In order to measure the thermoelectric response of the m2DEGs, an AC heating current  $I_h$  at frequency  $f_h = 11 \text{ Hz}$  was used to establish a temperature gradient along  $L$  which, being  $\propto I_h^2$ , alternates at  $2f_h$ . Thus the thermovoltage  $V_{\text{th}}$  was measured by locking-in to the second harmonic of  $I_h$ . The measurement of the temperature difference  $\Delta T$  across the m2DEG is described in detail in Refs. [12] and [14]. Briefly, this was done closely following the scheme initially demonstrated in Refs. [15,16] where lithographically defined thermocouples were used to measure the local electron temperature. As shown in Fig. 1a each thermocouple consisted of two long and gated 2DEG arms extending outwards from a location along the heated 2DEG and terminating in a ohmic contact each. The heated 2DEG area served as the 'hot junction' for a thermocouple and applying a differential voltage bias on the arms resulted in a measurable thermovoltage  $V_{\text{th}}^{\text{TC}}$  between the ohmic contacts.  $V_{\text{th}}^{\text{TC}}$  was related to the local electron temperature  $T_e$  as:

$$T_e^2 = V_{\text{th}}^{\text{TC}} \frac{6e\hbar^2}{\pi k_B^2 m(1 + \alpha)} \left( \frac{1}{n_1} - \frac{1}{n_2} \right)^{-1} + T_L^2 \quad (1)$$

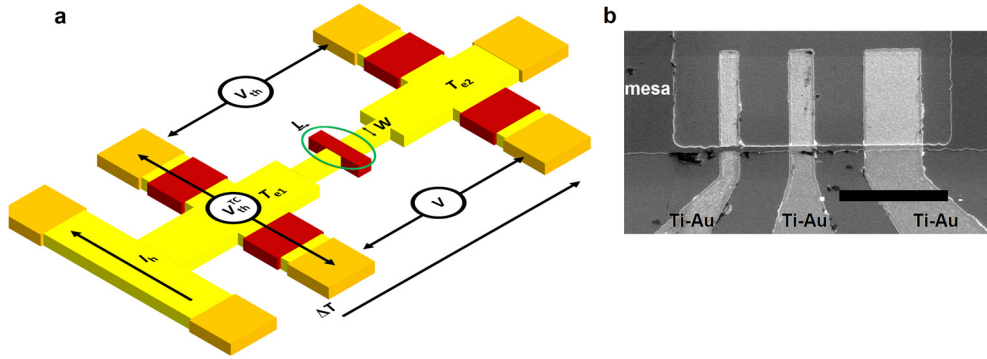


**Fig. 1.** (a) Schematic representation of devices. The yellow regions show the conducting mesa with the ohmic contacts for voltage/current measurements depicted in gold, and top-gate electrodes shown in red. The m2DEG of dimensions  $L \times W$  is highlighted in a green ellipse. We note that in addition to the m2DEG, there are ungated 2DEG sections that lie between the voltage probes which contribute an additional series resistance. However, the contribution from these sections is at most 5% of the m2DEG resistance in the  $V_g$ -values of interest, and can safely be ignored [10]. When required, a heating current  $I_h$  is used to establish a temperature gradient  $\Delta T$  along the direction shown. The local electron temperature is measured at the locations marked  $T_{e1}$  and  $T_{e2}$  using lithographically-defined thermocouples extending outwards from the specified locations. The thermovoltage  $V_{th}$  in response to  $I_h$  is measured across the m2DEG in parallel to  $V$  which is for the measurement of  $\rho$ . (b) An SEM of three m2DEGs with varying  $L$  defined in a channel with  $W = 3 \mu\text{m}$ . The scale bar shows  $20 \mu\text{m}$ .

Here  $m$  is the effective electron mass in GaAs ( $= 0.067m_0$ , where  $m_0$  is the bare electron mass),  $\alpha$  is given by  $(n_s/\tau)(d\tau/dn_s)$  where  $\tau$  is the elastic scattering time,  $n_1$  and  $n_2$  are the 2DEG densities beneath the two gated sections of the thermocouple respectively, and  $T_L$  is the lattice temperature obtained from a ruthenium oxide thermometer attached to the cold finger of the cryostat. Equation (1) is arrived at by invoking the Mott formula [17] which states that the diffusion thermopower or Seebeck coefficient  $S_D$  of a 2D conductor and its electrical conductivity  $\sigma$  are related as:

$$S_D = \frac{\pi^2 k_B^2 T}{3q} \left( \frac{d \ln \sigma}{dE} \right)_{E=\mu} \quad (2)$$

where  $q$  is the charge per unit carrier,  $E$  is the energy and  $\mu$  the chemical potential of the 2D conductor. In the specific case when  $\sigma = n_s e^2 m / \tau$ , where  $-e$  is the electronic charge, Equation (2) reduces to:

$$S_D = \frac{\pi k_B^2 T m}{3e \hbar^2} \frac{1 + \alpha}{n_s} \quad (3)$$

Equation (3) provides an analytical expression for  $S$  in a non-interacting, classical 2DEG, i.e. in which quantum and interaction effects are imperceptible, and we will use it as a benchmark to gauge the contribution due to electron–electron correlations and/or localisation.

### 3. Experimental results

In this section we will describe the electrical and thermoelectrical transport properties of m2DEGs. However, in order to appreciate the striking nature of experimental findings, we begin with a brief note on the behaviour of macroscopic 2DEGs. High- $n_s$  2DEGs in both Si-based MOSFETs and GaAs-based heterostructures show many outwardly metallic transport characteristics, most notable of which are  $d\rho/dT \geq 0$  [5–7] and a linear dependence of  $S$  on  $T$  [19]. While the existence of a 2D metallic phase would be in direct contradiction to the expectations of the scaling hypothesis of localisation [20,21], most if not all of the features of the ‘metallic’ phase can be understood within the framework of weak localisation (WL) as arising due to finite (but small)  $\ell_\phi$ . This in turn would imply that the true ground state of the 2DEG is electrically insulating, consistent with the expectations of the scaling hypothesis. As  $n_s$  is lowered, however, macroscopic 2DEGs are universally observed to crossover to the ‘Anderson localised’ or ‘strongly localised’ regime at  $\rho \approx h/e^2$  in which electron transport is via phonon-assisted ‘hops’. The  $n_s$  at which this so-called ‘2D MIT’ occurs is non-universal and in the range of  $10^{14} \text{ m}^{-2}$ , below which  $\rho \sim \exp(\Delta/k_B T)^p$ , with  $\Delta$  being the hopping energy, and the exponent  $p = 1, 1/2$  or  $1/3$  depending on the precise hopping mechanism [17]. The 2D MIT has been the subject of much debate, the central point of contention being whether the experimental data is indicative of a true  $n_s$ -driven quantum phase transition, or simply a disorder-driven crossover [22]. Crucially, however, regardless of the underlying mechanism, macroscopic 2DEGs are *always* observed to be in the strongly localised regime when  $\rho \gtrsim h/e^2$ , with both  $\rho$  and  $S$  diverging as  $T \rightarrow 0 \text{ K}$ . This is perhaps, the most striking distinction between macroscopic and mesoscopic 2DEGs.

Fig. 2 shows the low- $T$ -dependence of  $\rho$  and  $S$  of m2DEGs in the low- $n_s$  regime where  $\rho \gg h/e^2$ . In sharp contrast to macroscopic samples, and as was consistently reported in a number of works on m2DEGs [23,24,12,18,11,10,25], the activated growth of  $\rho(T)$  shows a striking slowing down below  $\approx 1 \text{ K}$ . As is seen in Fig. 2a,  $d\rho/dT$  is found to be  $\approx 0$  for  $T \lesssim 1 \text{ K}$ , with  $\rho$  appearing to saturate to a large albeit finite value as  $T \rightarrow 0 \text{ K}$ . This behaviour was found to be

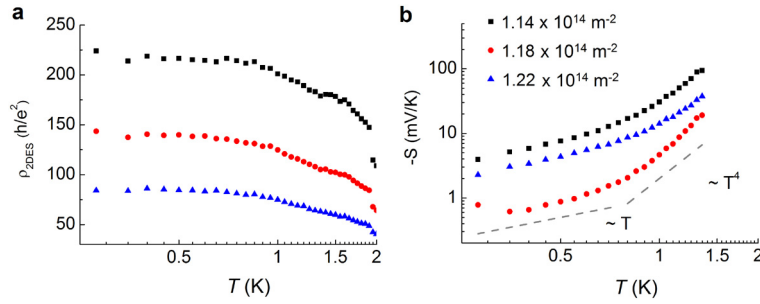


**Fig. 2.** (a) Even when nominally in the strongly localised regime the m2DEGs do not show activated-type behaviour characteristic of hopping transport. Instead,  $\rho$  is almost completely  $T$ -independent below  $\approx 1$  K. (b) In the same regime,  $S$  shows manifestly metal-like characteristics, although being orders of magnitude larger than conventionally expected (see Eq. (3)). Figure adapted from Ref. [12].

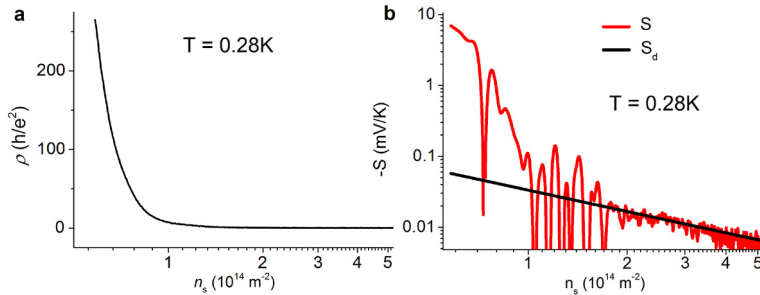


**Fig. 3.** The  $n_s$ -dependences of  $\rho$  and  $S$  are apparently in striking disagreement with the expectations of Eq. (2), while  $\rho$  is essentially monotonic in  $n_s$ ,  $S$  shows sharp oscillations and even sign-reversals. Figure adapted from Ref. [18].

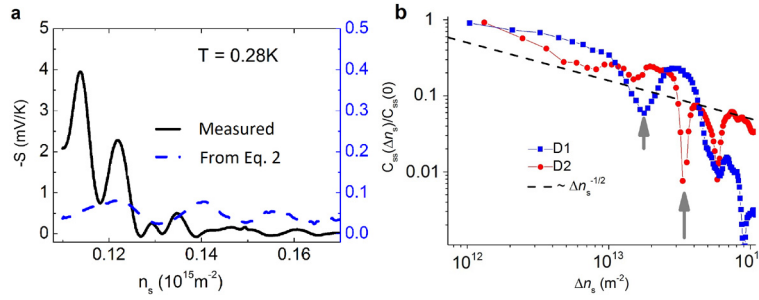
robust over a wide range of system parameters [23,24], as well as over a wide range of sample dimensions [10,25], only appearing to vanish in the macroscopic system limit [23]. We stress that this behaviour is totally at odds with anything observed in macroscopic 2DEGs which, when at comparable  $\rho$ , are deep within the Anderson localised regime with  $\rho$  being strongly  $T$ -dependent. On the other hand, of the several measured m2DEGs, *not a single one showed any indication of activated behaviour below  $\approx 1$  K*. That is, the low- $T$  saturation in  $\rho$  was not only seen in a selection of devices, but seen in every device measured.

Fig. 2b shows the  $T$ -dependence of  $S$  in the same range over which the saturation in  $\rho$  is observed, and it is found that  $S$  in m2DEGs grows linearly as a function of  $T$  extrapolating to zero at 0 K. This behaviour is qualitatively in agreement with that expected in non-interacting metals (see Eq. (3)). In terms of absolute magnitude, however,  $S$  was found to exceed the Mott value by over two orders of magnitude [12]. It is important to note that in the hopping regime  $S$  is expected to diverge as  $T \rightarrow 0$  K. The precise form of the divergence depends on the precise hopping mechanism, i.e. whether it is nearest-neighbour, variable-ranged or hopping in the presence of the Coulomb gap, but clearly this is totally inconsistent with the experimental observations in Fig. 2b. As  $T$  is increased above  $\approx 1$  K,  $\rho$  appears to decrease in a more conventional activated manner indicating a recovery of the hopping regime. On the other hand  $S$  is found to sharply increase as  $\sim T^4$  suggesting the role of electron–phonon interactions [26]. Notably, the rapid  $T^4$ -growth sees  $S$  attain enormously large values of  $\sim 100$  mV/K at 1 K, which are larger than any other previously reported value.

Thus, to briefly summarise the  $T$ -dependent characteristics, both  $\rho$  and  $S$  seem to suggest that the m2DEG has metal-like excitations below  $\approx 1$  K and even at the lowest accessible  $n_s$ , there seems to be no crossover to strongly localised behaviour. The magnitude of  $\rho$  and  $S$ , however, are significantly larger than is conventionally found in the high- $n_s$  ‘metallic’ regime of 2DEGs and we address this in Section 4 after inspecting the  $n_s$ -dependence below.

Fig. 3 shows the  $n_s$ -dependence of  $\rho$  and  $S$  [12,11]: it is observed that while  $\rho(n_s)$  increases essentially in a monotonic fashion,  $S$  is markedly non-monotonic showing large oscillations and even sign-changes as a function of  $n_s$ . The onset of  $S$ -oscillations was consistently found to occur in the vicinity of  $n_s = 1.8 \times 10^{14} \text{ m}^{-2}$ , above which  $S$  was found to agree quantitatively with the Mott prediction (Eq. (3)). Thus, in contrast with the low- $T$ -dependence, the low- $n_s$  behaviour appears to be in qualitative disagreement with the Mott prediction (Eq. (2)) which requires oscillations in  $S$  to be accompanied by oscillations in  $\rho$ . Notably in this context,  $\rho$  was found to be featureless to within the experimental resolution of a few ohms per square [11]. The apparent failure of the Mott picture is further brought out in Fig. 4a where the measured  $S$  is compared to  $S_{\text{Mott}}$  given by Eq. (2). Not only do  $S$  and  $S_{\text{Mott}}$  oscillate asynchronously, the former exceeds the latter by over two orders of magnitude.

Thus to summarise this section, the experimental data point at an unconventional metallic character in m2DEGs even when  $\rho \gg h/e^2$ , and which is never observed to give way to conventional hopping transport down to the lowest experimentally accessible  $n_s$  and/or  $T$ . That is, the m2DEGs seem to totally avoid the hopping regime below  $\approx 1$  K. In addition,



**Fig. 4.** (a) The measured  $S$  and that constructed using the measured  $\sigma$  and Eq. (2) disagree quantitatively and qualitatively. However, as was shown in Ref. [27] this behaviour is anticipated in phase-coherent systems and is a manifestation of ‘universal mesoscopic fluctuations’. (b) shows that the two-point correlation function of the  $S$  fluctuations (defined as the product  $\Delta S(n_{s,1})\Delta S(n_{s,2})$ , where  $\Delta S(n_s) = S(n_s) - S_d(n_s)$ ) is in strong agreement with the predictions of Ref. [27], decaying as  $\Delta n_s^{-1/2}$ , where  $\Delta n_s \equiv n_{s,1} - n_{s,2}$ . Figure adapted from Ref. [11].

$S$  in m2DEGs shows a dramatic departure from the Mott formula. These results are completely novel with no similar findings been reported in macroscopic 2DEGs. In the next section we argue that several of these unexpected results can be understood as arising due to phase coherent electron transport.

#### 4. Discussion: manifestations of phase coherence?

One of the most direct indications of phase coherent behaviour is the appearance of ‘universal mesoscopic fluctuations’ which are non-periodic but reproducible fluctuations in the transport as a function of an external parameter such as magnetic field or chemical potential. These arise due to the specific disorder realisation of the system under study which, in mesoscopic systems, tends not to be statistically homogeneous. Specifically, the trajectory followed by an electron, and therefore the net phase it accumulates, as it traverses a mesoscopic system, will depend sensitively on scattering events and thus the disorder profile. Since the disorder profile can change in an essentially random manner as the chemical potential is tuned, sharp changes in the electron-interference characteristics can be expected which ultimately manifest as fluctuations in the transport characteristics. In Ref. [11] it was shown that certain aspects of the  $S$ -oscillations shown in Fig. 3b were strongly consistent with theoretical predictions for mesoscopic  $S$  fluctuations [27]. In particular, Ref. [27] predicted that phase coherent systems should show very large  $S$ -oscillations, both positive and negative, and the autocorrelation function of the oscillations should decay as a power law with an exponent of  $-1/2$ , and go through a minimum before decaying completely. Remarkably, this is almost exactly what was found experimentally in Ref. [11] (see Fig. 4b). What is the physical origin of such large fluctuations? We note that any sharp changes in  $\sigma$ , such as universal conductance fluctuations (UCFs), will induce divergences in  $S$  due to the differential relation between  $\sigma$  and  $S$  in Eq. (2). Furthermore, these divergences can be negative or positive, and will be present even if the fluctuations in  $\sigma$  are very small, i.e. beyond experimental resolution, thus offering a plausible explanation for the seemingly contradictory observations in Figs. 3a and 3b. But this then leads to the question as to why no fluctuations are visible in Fig. 3a, i.e. why the fluctuations should be ‘beyond experimental resolution’ when UCFs are expected to be of magnitude  $\delta G \sim e^2/h$ , i.e.  $\delta R \sim R^2 e^2/h$ . While this remains an important open question, a naïve application of this expression would result in enormous  $\delta R$  in the regime where  $S$ -oscillations are visible, which are clearly not observed. More importantly, however, it is not *a priori* clear that this expression remains valid when  $R > h/e^2$ , and we are unaware of any theoretical framework that describes mesoscopic conductance fluctuations in this regime.

If indeed the mesoscopic size of the 2DEGs causes the fluctuations in  $S$ , then increasing the 2DEG size should reveal important information. In Ref. [10] it was shown that at strongly negative  $V_g$ , i.e. low  $n_s$ ,  $\rho$  in the m2DEGs had a marked dependence on the system size: as shown in Figs. 5a, 5b, and 5c, with the exception of a few non-monotonicities,  $\rho$  broadly appears to grow with increasing  $L$ . The expected  $L$ -independent behaviour is recovered as  $V_g$  is made less negative. The observation of similar behaviour in three separate devices (Figs. 5a, 5b, and 5c), and the reproducible nature of the observed behaviour [10], strongly disfavours any disorder-based explanation of the data. One possibility is that the localisation length  $\xi$  of the m2DEG is comparable to its spatial extent, thereby suppressing electron diffusivity and ultimately manifesting as a geometry-dependent  $\rho$ . In other words, it is conceivable that the m2DEGs are Anderson localised. While in itself not surprising, it is worth emphasising that the observation of Anderson localisation is strongly contingent on a well-defined  $\xi$  and therefore on electronic phase coherence over the lengthscales of interest. This is particularly remarkable in light of the data shown in Fig. 5d, which seems to indicate that the length-dependence is not completely suppressed even at 10 K! To further investigate the data, we construct in Fig. 5e the ‘ $\beta$ -function’  $\equiv d \ln(\sigma/\sigma_0)/d \ln L$ , where  $\sigma_0 = e^2/h$ , using pairs of points in Fig. 5c. Despite the considerable scatter (arising due to the discrete pairwise derivative operation), the data is broadly consistent with the known limiting values of  $\beta$  when  $\sigma \ll \sigma_0$  and  $\sigma \gg \sigma_0$ , respectively. Perhaps more interestingly, the data lies in the crossover regime between weak and strong localisation, which is theoretically more challenging to describe. Although system-size-dependent characteristics have been observed in other systems [28,29], we believe this is the first direct observation of behaviour consistent with the predictions of the scaling hypothesis.

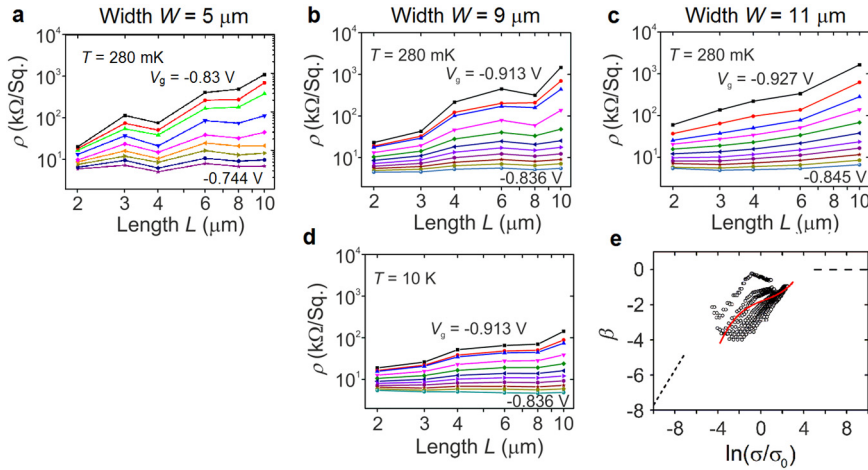


**Fig. 5.** (a)–(c) show  $\rho$  as a function of  $L$  for three sets of m2DEGs, each with a different  $W$ . Strikingly,  $\rho$  shows a systematic growth with  $L$  at large, negative  $V_g$ . (d) This behaviour is seen to persist, albeit to a lesser degree, up to relatively high  $T$  of 10 K. (e) From the  $L$ -dependent characteristics, we construct the ‘scaling function’  $\beta$  (defined in the text) and find it to be in reasonable agreement with the theoretically anticipated values (shown as broken lines) in the opposite limits  $\sigma \gg \sigma_0$  and  $\sigma \ll \sigma_0$ , respectively. The red trace is an average of the data points (open circles).

How would this tell on the  $T$ -dependence of transport? First, as  $T$  is increased it is to be expected that phase coherence and, therefore, the  $L$ -dependent behaviour diminishes. This is clearly seen in Fig. 5d which shows that the growth of  $\rho$  as a function of  $L$  is reduced at 10 K. Perhaps more subtle is the fact that if the electronic wavefunction extends coherently across the m2DEG, then the transport must be metal-like. This can be seen by noting that even though  $\xi$  is finite, this is irrelevant in systems with spatial extent  $\lesssim \xi$  in which the wavefunction would appear extended. Indeed, this is exactly what is observed in the m2DEGs at  $T \lesssim 1 \text{ K}$  with both  $\rho$  and  $S$  showing behaviour characteristic of metals (Fig. 2a and 2b, respectively). But if the system is effectively a metal, why is  $\rho$  so large in magnitude? The precise value of  $\rho$  depends on the diffusivity of electrons and this is vanishingly small on lengthscales  $> \xi$ . Importantly, on intermediate lengthscales  $\lesssim \xi$  the diffusivity will be diminished, but not zero. It was shown in Ref. [10] that the m2DEGs under consideration are precisely in this regime, with  $\xi \approx L$ . In fact, the low- $T$  saturation value of  $\rho$  is observed to increase monotonically with  $L$ , further supporting the picture of reduced electronic diffusivity with increasing  $L$ . The last remaining question is then why the metallic behaviour gives way to conventional hopping behaviour above  $\approx 1 \text{ K}$ . The point to note here is that irrespective of phase coherence, electrons are continually interacting with phonons, i.e. the hopping transport channel  $\sim \exp(\Delta/k_B T)$  is always present. As  $T$  is increased, the hopping contribution grows until it exceeds the coherent transport causing a decrease in  $\rho(T)$ . As shown in Ref. [10],  $\rho(T)$  in the m2DEGs can be fitted very well to a simple description in which the hopping and coherent channels constitute two parallel conduction paths.

Thus we see that several of the seemingly anomalous characteristics of the m2DEGs including the metal-like behaviour when  $\rho \gg h/e^2$  and the apparent breakdown of the Mott relation (Eq. (2)) can be understood as stemming from phase coherent electron transport. However, this is a very surprising conclusion since this would imply  $\ell_\phi \sim 10 \mu\text{m}$  even at 10 K which is many orders of magnitude greater than expected [13]. Alternatively, one could ask whether disorder could give rise to the observed effects [30–32], but the systematic nature of  $\rho(L)$  (reported for three independent sets of six m2DEGs each in Ref. [10]), the absence of Coulomb blockade features in very narrow m2DEGs [25], and the consistent observation of the low- $T$  metallic character in numerous 2DEGs [23,24,12,10,25] strongly argues against disorder-based scenarios. An entirely different argument could be whether the observed phenomena are, as was argued in Refs. [23,24,12,18], driven by many-body effects. This is particularly relevant in light of the large magnitude of  $S$  since, although intuitively a large  $\rho$  also implies a large  $S$ , the magnitude of  $S$  at low  $n_s$  ( $\lesssim 4 \times 10^{14} \text{ m}^{-2}$ ) is over an order of magnitude larger than predicted by Eq. (2). In this  $n_s$ -regime the interaction parameter  $r_s$ , defined as the ratio of the Coulomb energy of the system to its kinetic energy, can be as large as 8 and therefore interactions must play a prominent role. In this respect we point out two theoretical works which predict sign changes [33] or divergences [34] in  $S$  as a function of particle concentration arising due to the proximity to a quantum critical point and strong electron correlations, respectively. However, it is unclear whether these scenarios simultaneously predict a system-size dependence of the transport parameters and/or low- $T$  metal-like transport at very high  $\rho$ .

In summary, our recent experimental studies on m2DEGs of spatial extent less than  $10 \mu\text{m}$  provide strong indications of phase coherence transport even at  $T \approx 10 \text{ K}$ . This entirely unexpected result is based on a combination of electrical and thermoelectrical measurements on a wide range of m2DEGs of varying shape and dimension which show (1) metallic  $T$ -dependence of  $\rho$  and  $S$  below  $\approx 1 \text{ K}$  despite  $\rho \gg h/e^2$  [23,24,12], (2) an apparent decoupling of  $\rho$  and  $S$  wherein the latter oscillates but the former is monotonic as a function of  $n_s$  [18,11], and (3) a systematic dependence of  $\rho$  on the system-size which is strongly consistent with the predictions of the scaling hypothesis of localisation [10]. A consequence

of the mesoscopic nature of the 2DEGs is that  $S$  can attain enormously large values of up to 100 mV/K at 1.3 K [12], which can be very useful for thermoelectric applications at cryogenic temperatures.

## Acknowledgements

We gratefully acknowledge funding from the Engineering and Physical Sciences Research Council (EPSRC), UK and the Leverhulme Trust, UK.

## References

- [1] D.A. Wharam, T. Thornton, R. Newbury, M. Pepper, H. Ahmed, J.E.F. Frost, D.G. Hasko, D.C. Peacock, D.A. Ritchie, G.A.C. Jones, *J. Phys. C, Solid State Phys.* 21 (1988) L209.
- [2] B.J. van Wees, H. van Houten, C.W.J. Beenakker, J.G. Williamson, L.P. Kouwenhoven, D. van der Marel, C.T. Foxon, *Phys. Rev. Lett.* 60 (1988) 848.
- [3] C. Smith, M. Pepper, H. Ahmed, J. Frost, D. Hasko, D. Peacock, D. Ritchie, G.A.C. Jones, *J. Phys. C, Solid State Phys.* 21 (1988) L893.
- [4] B. van Wees, L. Kouwenhoven, C. Harmans, J. Williamson, C. Timmering, M. Broekaart, C. Foxon, J. Harris, *Phys. Rev. Lett.* 62 (1989) 2523.
- [5] M.Y. Simmons, A.R. Hamilton, M. Pepper, E.H. Linfield, P.D. Rose, D.A. Ritchie, *Phys. Rev. Lett.* 84 (2000) 2489.
- [6] A.R. Hamilton, M.Y. Simmons, M. Pepper, E.H. Linfield, D.A. Ritchie, *Phys. Rev. Lett.* 87 (2000) 126802.
- [7] E. Abrahams, S.V. Kravchenko, M.P. Sarachik, *Rev. Mod. Phys.* 73 (2001) 251.
- [8] K. v. Klitzing, G. Dorda, M. Pepper, *Phys. Rev. Lett.* 45 (1980) 494.
- [9] D.C. Tsui, H.L. Stormer, A.C. Gossard, *Phys. Rev. Lett.* 48 (1982) 1559.
- [10] D. Backes, R. Hall, M. Pepper, H. Beere, D. Ritchie, V. Narayan, *Phys. Rev. B* 92 (2015) 235427.
- [11] V. Narayan, E. Kogan, C. Ford, M. Pepper, M. Kaveh, J. Griffiths, G. Jones, H. Beere, D. Ritchie, *New J. Phys.* 16 (2014) 085009.
- [12] V. Narayan, M. Pepper, J. Griffiths, H. Beere, F. Sfigakis, G. Jones, D. Ritchie, A. Ghosh, *Phys. Rev. B* 86 (2012) 125406.
- [13] T. Heinzel, *Mesoscopic Electronics in Solid State Nanostructures*, Wiley-VCH, Weinheim, Germany, 2007.
- [14] J. Billiard, D. Backes, J. König, I. Farrer, D. Ritchie, V. Narayan, *Appl. Phys. Lett.* 107 (2015) 022104.
- [15] R. Syme, M. Kelly, M. Pepper, *J. Phys. Condens. Matter* 1 (1989) 3375.
- [16] W.E. Chickering, J.P. Eisenstein, J.L. Reno, *Phys. Rev. Lett.* 103 (2009) 046807.
- [17] N.F. Mott, E.A. Davis, *Electronic Processes in Non-Crystalline Materials*, Clarendon Press, Oxford, UK, 1971.
- [18] V. Narayan, M. Pepper, J. Griffiths, H. Beere, F. Sfigakis, G. Jones, D. Ritchie, A. Ghosh, *J. Low Temp. Phys.* 171 (2013) 626.
- [19] R. Fletcher, V.M. Pudalov, A.D.B. Radcliffe, C. Possanzini, *Semicond. Sci. Technol.* 16 (2001) 386.
- [20] E. Abrahams, P.W. Anderson, D.C. Licciardello, T.V. Ramakrishnan, *Phys. Rev. Lett.* 42 (1979) 673.
- [21] P.A. Lee, T.V. Ramakrishnan, *Rev. Mod. Phys.* 57 (1985) 287.
- [22] S.D. Sarma, M.P. Lilly, E.H. Hwang, L.N. Pfeiffer, K.W. West, J.L. Reno, *Phys. Rev. Lett.* 94 (2005) 136401.
- [23] M. Baenninger, A. Ghosh, M. Pepper, H.E. Beere, I. Farrer, D.A. Ritchie, *Phys. Rev. Lett.* 100 (2008) 016805.
- [24] R. Koushik, M. Baenninger, V. Narayan, S. Mukerjee, M. Pepper, I. Farrer, D.A. Ritchie, A. Ghosh, *Phys. Rev. B* 83 (2011) 085302.
- [25] D. Backes, R. Hall, M. Pepper, H. Beere, D. Ritchie, V. Narayan, *J. Phys. Condens. Matter* 28 (2016) 1LT01.
- [26] S.K. Lyo, *Phys. Rev. B* (R) 38 (1989) 6345.
- [27] G. Lesovik, D. Khmel'nitskii, *Sov. Phys. JETP* 67 (1988) 957.
- [28] D. Bishop, G. Dolan, *Phys. Rev. Lett.* 55 (1985) 2911.
- [29] D. Popović, A. Fowler, S. Washburn, *Phys. Rev. Lett.* 67 (1992) 2870.
- [30] V. Tripathi, M.P. Kennett, *Phys. Rev. B* 74 (2006) 195334.
- [31] V. Tripathi, M.P. Kennett, *Phys. Rev. B* 76 (2007) 115321.
- [32] D. Neilson, A.R. Hamilton, *Phys. Rev. B* 84 (2011) 129901.
- [33] A. Garg, B.S. Shastri, K.B. Dave, P. Phillips, *New J. Phys.* 13 (2011) 083032.
- [34] K. Limragool, P.W. Phillips, *Phys. Rev. Lett.* 113 (2014) 086405.